STUDY OF PRODUCTION OF OPEN HEAVY FLAVOR HADRONS THROUGH THEIR SEMI-LEPTONIC DECAYS AT RHIC AND LHC*

Wei Xie

Department of Physics, Purdue University
525 Northwestern Ave., West Lafayette, IN 47907, USA
wxie@purdue.edu

(Received December 5, 2011)

I review the status of studying open heavy flavor production at RHIC and the LHC focusing on the results from non-photonic electron production. I compare the measurements with theoretical predictions and discuss the current understanding of heavy quark production in the strongly-coupled QGP produced in heavy-ion collisions.

DOI:10.5506/APhysPolB.43.671
PACS numbers: 13.20.Fc, 13.20.He, 25.75.Cj

1. Introduction

Heavy quarks are unique probes to study the strongly-coupled quark-gluon plasma created at RHIC and LHC. Unlike light quarks, heavy quark masses come mostly from spontaneous symmetry breaking, which makes them ideal for studying the QCD properties of the medium. Due to their large masses, they are produced early in collisions and are expected to interact with the medium quite differently from light quarks. Detailed studies of the production of open heavy flavor hadrons in heavy-ion collisions provide crucial information on understanding the medium properties.

Open heavy-flavor production can be studied directly by reconstructing charm and bottom hadrons through their hadronic decays or indirectly by measuring leptons from charm and bottom hadron decays, *e.g.*, non-photonic electrons. While providing indirect access to the original kinematics of the heavy quarks, the lepton measurements are more advantageous in terms of higher branching ratios and they are facilitated by fast online triggers that extend the measurements to higher p_{T}.

* Presented at the Conference "Strangeness in Quark Matter 2011", Kraków, Poland, September 18–24, 2011.

In this article, I first discuss briefly the current theoretical understanding of the heavy quark energy loss mechanism. Then, I highlight a few experimental results at RHIC and the LHC and compare the measurements with model predictions. At the end, I provide a summary and present my outlook on the near future of open heavy flavor measurements at RHIC and the LHC.

2. Theoretical predictions on heavy quark energy loss

The observed strong suppression of high p_{T} light hadron production at RHIC is understood to arise from the energy loss from the gluon radiation [1]. Heavy quark energy loss was expected to be much smaller due to the smaller acceleration under the same kick from the medium constituents leading to lower amount of radiation ("dead cone effect" [2]). To explain the observed large suppression of non-photonic electron production at RHIC [3], other energy loss mechanisms, such as collisional energy loss where heavy quarks lose energy to the medium through elastic collisions [4], collisional dissociation of heavy flavor hadrons inside the medium [5], and the AdS/CFT gravity dual models [6] have been proposed.

Figure 1 shows some of the predictions at RHIC and the LHC. The upper panels are the prediction from the relativistic Langevin simulation on the R_{AA} as a function of p_{T} for charm quarks and bottom quarks in 200 GeV Au+Au (left) and 5.5 TeV Pb+Pb collisions (right) [4, 7]. Compared to the bottom quark production, the model predicts much larger suppression of the charm quark production at $p_{\mathrm{T}} = 2$–$5\,\mathrm{GeV}/c$. The overall trend of the charm and bottom R_{AA} as a function of p_{T} is also different. The middle panels of Fig. 1 show the predictions from AdS/CFT model and pQCD WHDG/DGLV model including both radiative and collisional energy loss for the charm (left) and bottom quark (right) R_{AA} as a function of p_{T} in 5.5 TeV Pb+Pb collisions with the gluon density from the PHOBOS extrapolation ($\frac{dN_g}{dy} = 1750$) and the KLN model of CGC ($\frac{dN_g}{dy} = 2900$) [7]. As in the Langevin simulation, these models also predict a different trend of R_{AA} as a function of p_{T} for charm and bottom productions. Another feature is that the pQCD model predicts that R_{AA} decreases as a function of p_{T} for $p_{\mathrm{T}} < 20\,\mathrm{GeV}/c$ and then changes the shape and increases as a function of p_{T}, while AdS/CFT model predicts that R_{AA} decreases only slightly at high p_{T}. This difference is amplified by taking the ratio of the charm R_{AA} to the bottom R_{AA} and can be measured in the near future. The lower panels show the predictions of the B and D meson R_{AA} as functions of p_{T} in 200 GeV Au+Au collisions (left) and 5.5 TeV Pb+Pb collision (right) from the model based on a light-cone wavefunction approach including collisional dissociation [5, 7]. The unique feature of the prediction is that the charm and bottom suppression factor are similar at $p_{\mathrm{T}} > 5\,\mathrm{GeV}/c$.

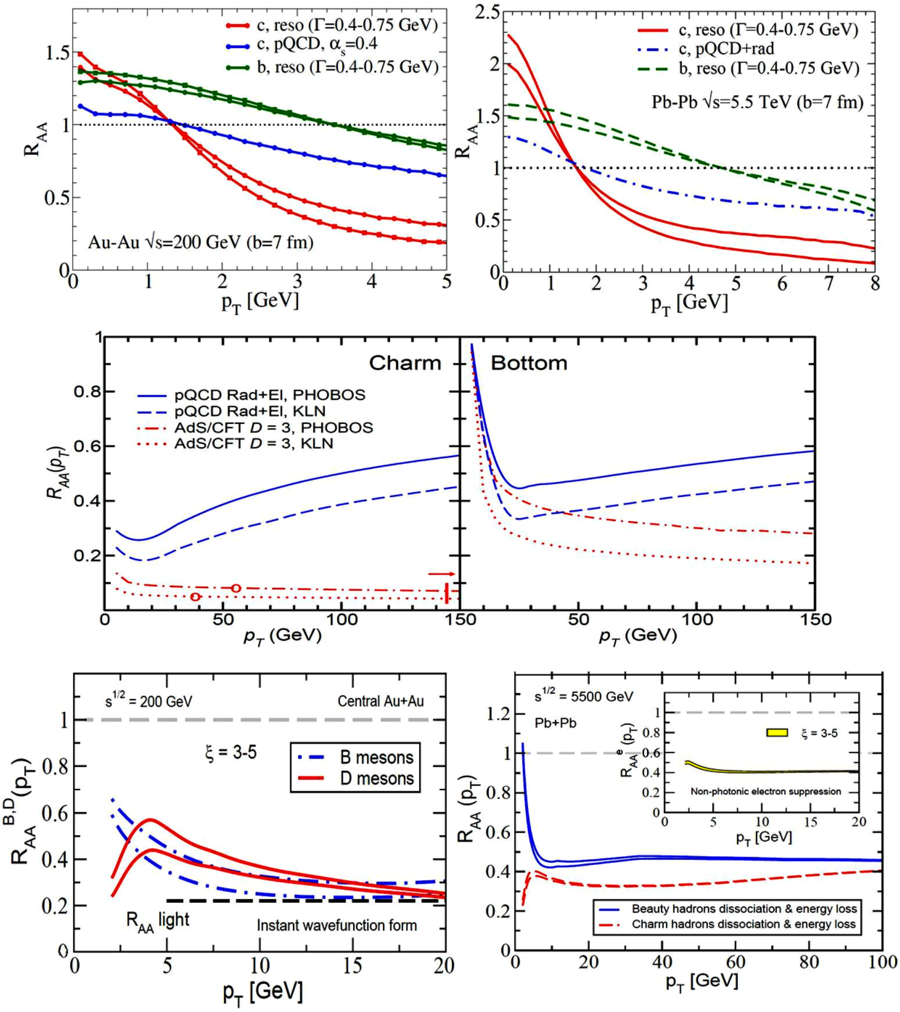

Fig. 1. Predictions of different heavy quark energy loss models at RHIC and LHC. See the text for details.

From the experimental point of view, we can take advantage of these features and disentangle charm and bottom production to discriminate among different production mechanisms.

3. Measurements at RHIC and LHC

Figure 2 shows the non-photonic electron measurements at RHIC [3] together with the predictions from different models [2, 4, 5, 6]. The measurements indicate that the non-photonic electron production at high p_{T}

is suppressed to the level of high p_{T} charged hadron productions. The WHDG/DGLV model, which can describe the light hadron suppression with only the radiative energy loss and $\frac{dN_g}{dy} = 1000$ (dashed line), underestimates the non-photonic electron R_{AA} at high p_{T}. After including the collisional energy loss (solid line), the result is closer to the data but is still unable to describe the data. On the other hand, the WHDG/DGLV prediction for charm quark only (long dashed line) agrees with the data quite well. The BDMPS model (dotted line) with $\hat{q} = 10\,\mathrm{GeV}^2/\mathrm{fm}$ can describe the light hadron R_{AA} but underestimates the non-photonic electron R_{AA} at high p_{T} and overestimates the measurements at low p_{T}. Both calculations from the relativistic Langevin simulation (dot-dashed line) and the model with collisional dissociation (dot-dot-dashed line) agree with the data very well at all p_{T}. The AdS/CFT model prediction is consistent with the measurement at high p_{T}.

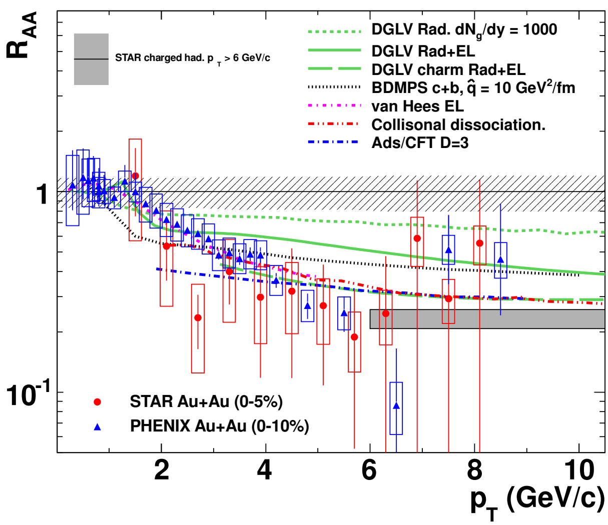

Fig. 2. Measurements of non-photonic electron R_{AA} as a function of p_{T} in 200 GeV Au+Au collisions from STAR (closed circles) and PHENIX (closed triangles). The band represents the STAR charged hadron measurement at $p_{\mathrm{T}} > 6\,\mathrm{GeV}/c$. Various lines represent predictions from different models. See the text for details.

Therefore, models with different or similar energy loss mechanisms can or cannot describe the data at RHIC. It is now critical to provide more differential measurements, especially the separate measurements on charm and bottom production as discussed in Sec. 2, for different collision energies to further understand the heavy quark interaction with the medium. This is becoming a reality as the LHC data are being analyzed and the RHIC detector is being upgraded.

Figure 3 shows the ALICE measurements of the non-photonic electron D^0 and D^+ meson nuclear modification factor in 2.76 TeV Pb+Pb collisions [8]. These are the first measurements done at higher-than-RHIC energies. The non-photonic electron R_{AA} as a function of p_{T} seems to be similar to that observed at RHIC but the result is overwhelmed by systematic errors which are dominated by TPC particle identification (35%) and cocktail inputs (25%). The D meson measurements are compared with some model predictions. The ASW model calculation includes only radiative energy loss with $\hat{q} = 25$–$100\,\mathrm{GeV}^2/\mathrm{fm}$ and is represented by the region between the lower solid and dashed lines. The WHDG/DGLV model prediction, with $dN_g/dy = 2200$–3500, includes both radiative and collisional energy loss and is represented as the region between the middle solid and dashed lines. The model based on the light-cone wavefunction approach with and without collisional dissociation is represented as the region between the upper solid and dashed lines. Among these predictions, ASW and the model based on the light-cone wavefunction approach are for 5.5 TeV Pb+Pb collisions. The WHDG/DGLV calculations are for 2.76 TeV Pb+Pb collisions and seem to be favored by this measurement.

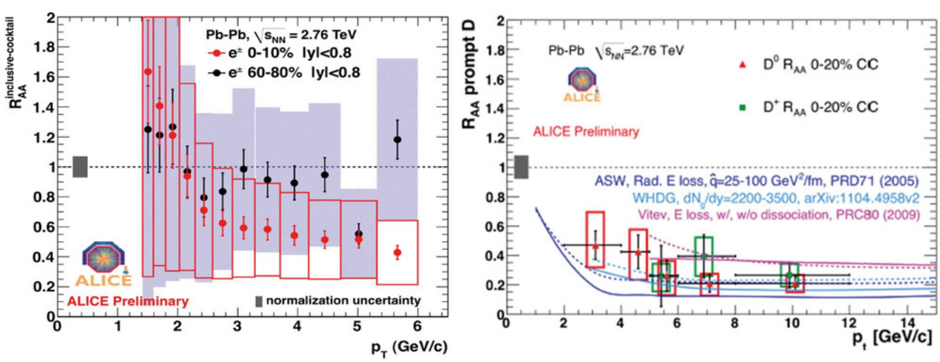

Fig. 3. ALICE measurements of non-photonic electron R_{AA} in central (0–10%) and peripheral (60–80%) collisions (left panel) and D meson R_{AA} in 0–20% collisions (right panel) as a function of p_{T} at $\sqrt{s_{NN}} = 2.76\,\mathrm{TeV}$. Model predictions are represented as lines. See the text for details.

In cases when the precise secondary vertex determination is not available, the contribution to the non-photonic electrons from bottom and charm hadron decays can be disentangled utilizing their different decay kinematics. In STAR, this is done through measuring the azimuthal correlation between non-photonic electrons and charged hadrons (e–h) as well as the correlation between non-photonic electrons and D^0 (e–D^0) [9]. The distribution of the azimuthal angle between non-photonic electrons and charged hadrons from bottom hadron decays is much wider than that from charm hadron decays as shown in the upper-left panel of Fig. 4. Through fitting the data with a function combining the two different distributions, one can obtain the contribution of bottom-decay electron to the non-photonic electron yield. As shown in the low-left panel of the Fig. 4, about 30–60% of non-photonic electrons come from bottom hadron decay at $p_{\mathrm{T}} > 3.0\,\mathrm{GeV}/c$ in 200 GeV $p+p$ collisions. The right panel of Fig. 4 shows the invariant cross section of bottom-decay and charm-decay electrons ($\frac{e^{+}+e^{-}}{2}$) as a function of p_{T} and the corresponding FONLL predictions, along with the ratio of each measurement to the FONLL calculations [10]. The results are obtained by multiplying the non-photonic electron spectra with the ratio of the bottom-decay electron yield to the non-photonic electron yield. In principle, the similar analysis can be done in Au+Au collisions, in which case we will be able to measure the R_{AA} for charm and bottom decay electron separately. In reality it is much more difficult in Au+Au collision because of large backgrounds. The silicon detector upgrade is needed to accomplish these measurements at RHIC.

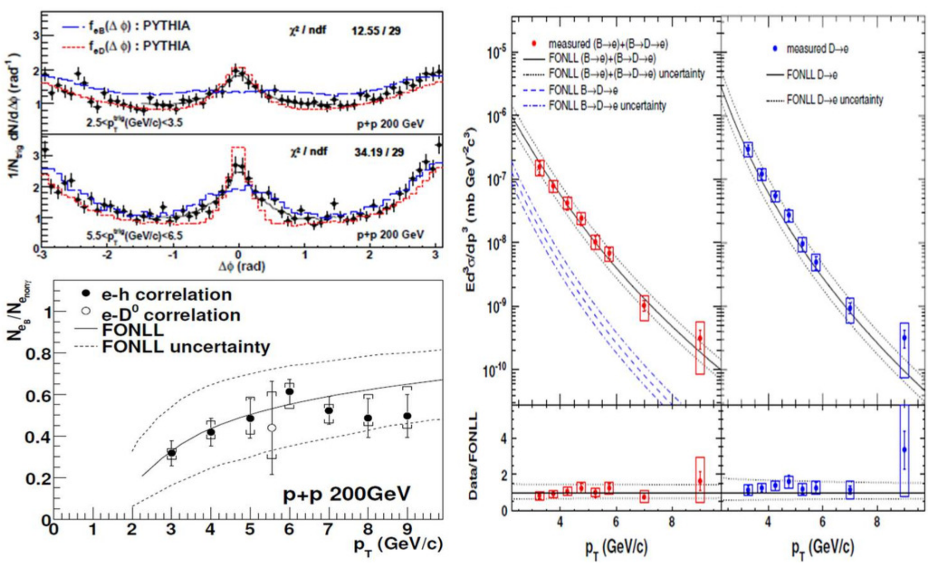

Fig. 4. Measurements of bottom-decay and charm-decay electron at RHIC in 200 GeV $p+p$ collisions. See the text for details.

The left panel of Fig. 5 shows the CMS result of bottom hadron R_{AA} as a function of N_{part} from $B \to J/\psi$ measurements in 2.76 TeV minimum-bias Pb+Pb collisions [11]. This is the first measurement showing directly that bottom production is significantly suppressed in the strongly-coupled QGP. The right panel of Fig. 5 shows the contours, with 90% confidence level, of nuclear modification factor for electrons from charm and bottom meson decays in 200 GeV central Au+Au collisions at RHIC [9]. This is obtained by combining the measurement of relative bottom-decay electron contribution to the non-photonic electron in $p + p$ collisions and R_{AA} measurement in Au+Au collisions [3]. Even in the extreme case where $R_{AA}^{eD} = 0$, $R_{AA}^{eB} \sim 0.6$ at 90% confidence level indicating bottom meson production is suppressed at high p_{T} in the most central Au+Au collisions. One immediate question is if the p_{T} region, where the bottom production is suppressed are the same at RHIC and at the LHC. Using PYTHIA6 with default settings, I compared the B meson p_{T} distribution when the decay electron $p_{\mathrm{T}} > 5\,\mathrm{GeV}/c$ and when the decay J/ψ $p_{\mathrm{T}} > 6\,\mathrm{GeV}/c$, *i.e.*, matching the cuts in each analysis, and found that the B meson p_{T} distribution in both cases peaks at around $10\,\mathrm{GeV}/c$ with majority of the counts in between 5 and $20\,\mathrm{GeV}/c$. It thus indicates that bottom production in the medium created at RHIC and LHC is significantly suppressed at $p_{\mathrm{T}} = 5$–$20\,\mathrm{GeV}/c$.

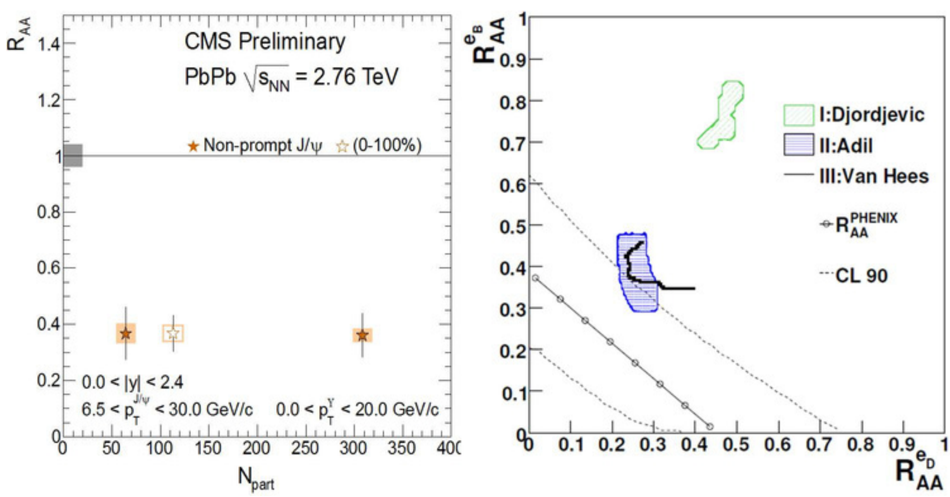

Fig. 5. CMS result of the bottom hadron R_{AA} as a function of N_{part} from $B \to J/\psi$ measurements at $\sqrt{s_{NN}} = 2.76\,\mathrm{TeV}$ (left). Confidence level contours of R_{AA} for electrons from charm (R_{AA}^{eD}) and bottom (R_{AA}^{eB}) meson decays at $p_{\mathrm{T}} > 5.0\,\mathrm{GeV}/c$ in 0–10% central Au+Au collisions at $\sqrt{s_{NN}} = 200\,\mathrm{GeV}$ (right).

4. Summary and outlook

The non-photonic electron measurements at RHIC have posed serious challenges to the theoretical understanding of the energy loss mechanism in the strongly-coupled QGP. One key input to discriminate among different mechanisms is to disentangle charm and bottom production. At the LHC, with silicon detectors already in place, the highest priority would be to reduce the systematic errors of the existing measurements and accumulate more luminosities. At RHIC, besides the luminosity upgrade, both STAR and PHENIX make vigorous efforts to upgrade their detectors [12]. PHENIX has already committed the barrel silicon detector in the last run and we will probably see the direct charm and bottom measurements at RHIC soon. In the mean time, I am looking forward to more novel measurements which were not possible before. One such measurement is the production and correlation of heavy-flavor jet where the leptons including both electrons and muons will play essential roles in tagging these jets.

REFERENCES

[1] M. Gyulassy, I. Vitev, X. Wang, B. Zhang, `arXiv:nucl-th/0302077v2`.

[2] D. Kharzeev *et al.*, *Phys. Lett.* **B561**, 93 (2003); N. Armesto *et al.*, *Phys. Lett.* **B637**, 362 (2006).

[3] A. Adare *et al.* [PHENIX Collaboration], *Phys. Rev. Lett.* **98**, 172301 (2007); B.I. Abelev *et al.* [STAR Collaboration], *Phys. Rev. Lett.* **106**, 159902 (2011).

[4] M. Djordjevic *et al.*, *Phys. Lett.* **B632**, 81 (2006); H. Van Hees *et al.*, *Phys. Rev. Lett.* **100**, 192301 (2008); P.B. Gossiaux *et al.*, *Nucl. Phys.* **A830**, 203 (2009); X. Zhao *et al.*, *Phys. Rev.* **C82**, 064905 (2010).

[5] R. Sharma *et al.*, *Phys. Rev.* **C80**, 054902 (2009).

[6] J.M. Maldacena, *Adv. Theor. Math. Phys.* **2**, 231 (1998); W.A. Horowitz *et al.*, *J. Phys. G* **35**, 104152 (2008).

[7] S. Abreu *et al.*, *J. Phys. G* **35**, 054001 (2008).

[8] F. Prino [ALICE Collaboration], *Acta Phys. Pol. B* **43**, 497 (2012), this issue.

[9] M.M. Aggarwal *et al.* [STAR Collaboration], *Phys. Rev. Lett.* **105**, 202301 (2010).

[10] H. Agakishiev *et al.* [STAR Collaboration], *Phys. Rev.* **D83**, 052006 (2011).

[11] B. Hong [CMS Collaboration], *Acta Phys. Pol. B* **43**, 517 (2012), this issue.

[12] J. Bouchet [STAR Collaboration], *Nucl. Phys.* **A830**, 636c (2009); L. Ruan *et al.*, *J. Phys. G* **36**, 095001 (2009); H. Ohnishi [PHENIX Collaboration], *Nucl. Instrum. Methods* **A569**, 33 (2006).